TABLE 8-3

Summary of TE^z_{mn} and TM^z_{mn} mode characteristics of rectangular waveguide

	$TE^z_{mn}\begin{pmatrix} m = 0,1,2,\dots \\ n = 0,1,2,\dots \end{pmatrix} \; m = n \neq 0$	$TM^z_{mn}\begin{pmatrix} m = 1,2,3,\dots \\ n = 1,2,3,\dots \end{pmatrix}$
E_x^+	$A_{mn}\dfrac{n\pi}{b\varepsilon}\cos\left(\dfrac{m\pi}{a}x\right)\sin\left(\dfrac{n\pi}{b}y\right)e^{-j\beta_z z}$	$-B_{mn}\dfrac{m\pi\beta_z}{a\omega\mu\varepsilon}\cos\left(\dfrac{m\pi}{a}x\right)\sin\left(\dfrac{n\pi}{b}y\right)e^{-j\beta_z z}$
E_y^+	$-A_{mn}\dfrac{m\pi}{a\varepsilon}\sin\left(\dfrac{m\pi}{a}x\right)\cos\left(\dfrac{n\pi}{b}y\right)e^{-j\beta_z z}$	$-B_{mn}\dfrac{n\pi\beta_z}{b\omega\mu\varepsilon}\sin\left(\dfrac{m\pi}{a}x\right)\cos\left(\dfrac{n\pi}{b}y\right)e^{-j\beta_z z}$
E_z^+	0	$-jB_{mn}\dfrac{\beta_c^2}{\omega\mu\varepsilon}\sin\left(\dfrac{m\pi}{a}x\right)\sin\left(\dfrac{n\pi}{b}y\right)e^{-j\beta_z z}$
H_x^+	$A_{mn}\dfrac{m\pi\beta_z}{a\omega\mu\varepsilon}\sin\left(\dfrac{m\pi}{a}x\right)\cos\left(\dfrac{n\pi}{b}y\right)e^{-j\beta_z z}$	$B_{mn}\dfrac{n\pi}{b\mu}\sin\left(\dfrac{m\pi}{a}x\right)\cos\left(\dfrac{n\pi}{b}y\right)e^{-j\beta_z z}$
H_y^+	$A_{mn}\dfrac{n\pi\beta_z}{b\omega\mu\varepsilon}\cos\left(\dfrac{m\pi}{a}x\right)\sin\left(\dfrac{n\pi}{b}y\right)e^{-j\beta_z z}$	$-B_{mn}\dfrac{m\pi}{a\mu}\cos\left(\dfrac{m\pi}{a}x\right)\sin\left(\dfrac{n\pi}{b}y\right)e^{-j\beta_z z}$
H_z^+	$-jA_{mn}\dfrac{\beta_c^2}{\omega\mu\varepsilon}\cos\left(\dfrac{m\pi}{a}x\right)\cos\left(\dfrac{n\pi}{b}y\right)e^{-j\beta_z z}$	0
β_c	$\sqrt{\beta_x^2+\beta_y^2} = \sqrt{\left(\dfrac{m\pi}{a}\right)^2+\left(\dfrac{n\pi}{b}\right)^2}$	
f_c	$\dfrac{1}{2\pi\sqrt{\mu\varepsilon}}\sqrt{\left(\dfrac{m\pi}{a}\right)^2+\left(\dfrac{n\pi}{b}\right)^2}$	
λ_c	$\dfrac{2\pi}{\sqrt{\left(\dfrac{m\pi}{a}\right)^2+\left(\dfrac{n\pi}{b}\right)^2}}$	
$\beta_z \; (f \geq f_c)$	$\beta\sqrt{1-\left(\dfrac{f_c}{f}\right)^2}$	
$\lambda_g \; (f \geq f_c)$	$\dfrac{\lambda}{\sqrt{1-\left(\dfrac{f_c}{f}\right)^2}} = \dfrac{\lambda}{\sqrt{1-\left(\dfrac{\lambda}{\lambda_c}\right)^2}}$	
$v_p \; (f \geq f_c)$	$\dfrac{v}{\sqrt{1-\left(\dfrac{f_c}{f}\right)^2}} = \dfrac{v}{\sqrt{1-\left(\dfrac{\lambda}{\lambda_c}\right)^2}}$	
$Z_w \; (f \geq f_c)$	$\dfrac{\eta}{\sqrt{1-\left(\dfrac{f_c}{f}\right)^2}} = \dfrac{\eta}{\sqrt{1-\left(\dfrac{\lambda}{\lambda_c}\right)^2}}$	$\eta\sqrt{1-\left(\dfrac{f_c}{f}\right)^2} = \eta\sqrt{1-\left(\dfrac{\lambda}{\lambda_c}\right)^2}$
$Z_w \; (f \leq f_c)$	$j\dfrac{\eta}{\sqrt{1-\left(\dfrac{f_c}{f}\right)^2}} = j\dfrac{\eta}{\sqrt{1-\left(\dfrac{\lambda}{\lambda_c}\right)^2}}$	$-j\eta\sqrt{1-\left(\dfrac{f_c}{f}\right)^2} = -j\eta\sqrt{1-\left(\dfrac{\lambda}{\lambda_c}\right)^2}$

	$TE^z_{mn}\begin{pmatrix} m = 0,1,2,\dots \\ n = 0,1,2,\dots \end{pmatrix} \; m = n \neq 0$	$TM^z_{mn}\begin{pmatrix} m = 1,2,3,\dots \\ n = 1,2,3,\dots \end{pmatrix}$
$(\alpha_c)_{mn}$	$\dfrac{2R_s}{b\eta\sqrt{1-\left(\dfrac{f_{c,mn}}{f}\right)^2}}\left\{\left(\varepsilon_m+\varepsilon_n\dfrac{b}{a}\right)\left(\dfrac{f_{c,mn}}{f}\right)^2 + \dfrac{b}{a}\left[1-\left(\dfrac{f_{c,mn}}{f}\right)^2\right]\dfrac{m^2ab+(na)^2}{(mb)^2+(na)^2}\right\}$ where $\varepsilon_p = \begin{cases} 2 & p=0 \\ 1 & p\neq 0 \end{cases}$	$\dfrac{2R_s}{ab\eta\sqrt{1-\left(\dfrac{f_{c,mn}}{f}\right)^2}}\dfrac{m^2b^3+n^2a^3}{(mb)^2+(na)^2}$

Table 8.7
Summary of Wave Types for Rectangular Guides[a]

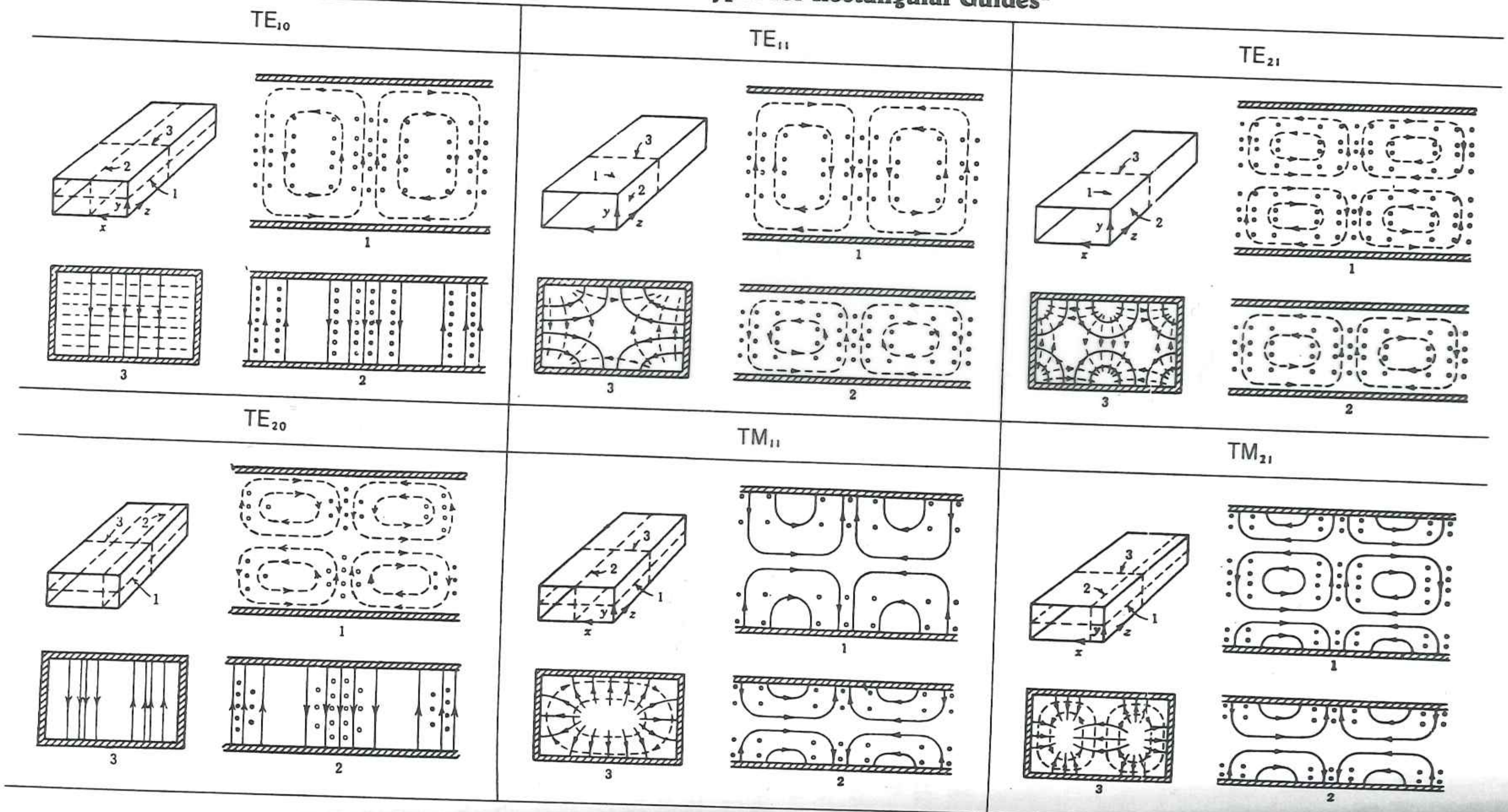

[a] Electric field lines are shown solid and magnetic field lines are dashed.

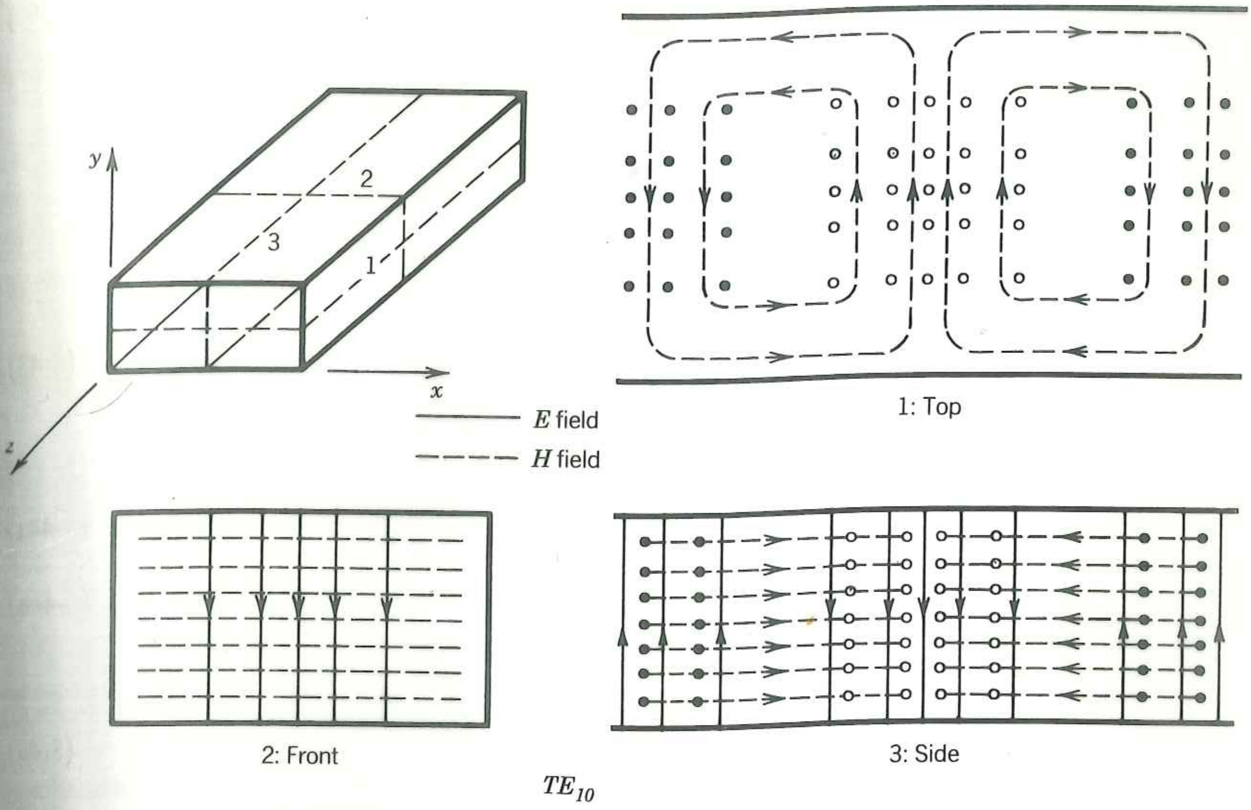

FIGURE 8-5 Electric field patterns for TE_{10} mode in a rectangular waveguide (*Source:* S. Ramo, J. R. Whinnery, and T. Van Duzer, *Fields and Waves in Communication Electronics*, 1984. Reprinted with permission of John Wiley & Sons, Inc.)

From the preceding information it is evident that the electric field intensity inside the guide has only one component, an E_y. The E- and H-field variations on the top, front, and side views of the guide are shown graphically in Figure 8-5, and the current density and H-field lines on the top and side views are shown in Figure 8-6 [2]. It is instructive at this time to examine the electric field intensity a little closer and attempt to provide some physical interpretation of the propagation

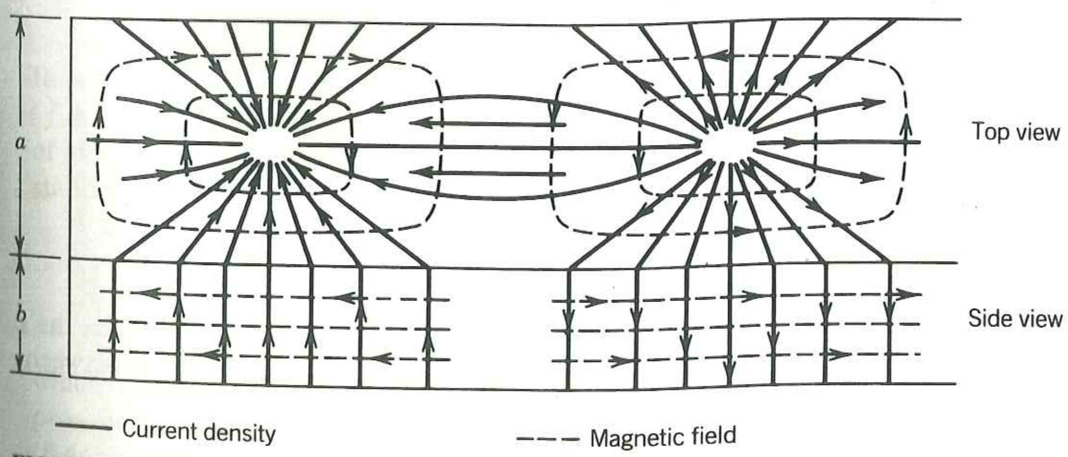

FIGURE 8-6 Magnetic field and electric current density patterns for the TE_{10} mode in a rectangular waveguide. (*Source:* S. Ramo, J. R. Whinnery, and T. Van Duzer, *Fields and Waves in Communication Electronics*, 1984. Reprinted with permission of John Wiley & Sons, Inc.)

8.2(15) and 8.2(16) are

(24)

(25)

k_y have the same forms
haracteristics for a TE_{mn}
der TM_{mn} mode. That is,
Modes that have different
be *degenerate modes.*
TE modes. Since electric
ch one of the TE modes
ndary and end on charges
gnetic field lines surround
erse electric fields. For the
ctric fields go between top
elds lie entirely in planes
t that it will be discussed

equencies of several of the
ant TE_{10} mode for a guide
d in most practical guides.
ency for the TE_{10} mode is
is way only one mode can
gation is avoided. Also, by
ed by having different group
al is minimized for the one
he entrance to the guide but
ort distance from the source.

3

tangular guide ($b/a = \frac{1}{2}$).

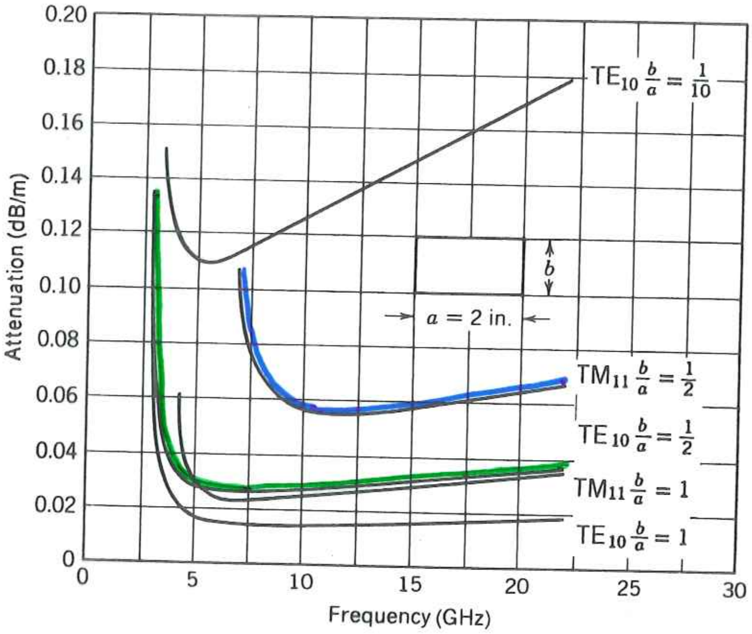

FIG. 8.7c Attenuation due to copper losses in rectangular waveguides of fixed width.

The attenuation constant for TE_{mn} ($n \neq 0$) modes is found using power transfer and power loss per unit length as in Eq. 8.5(11).

$$(\alpha_c)_{TE_{mn}} = \frac{2R_s}{b\eta\sqrt{1 - (f_c/f)^2}} \left\{ \left(1 + \frac{b}{a}\right)\left(\frac{f_c}{f}\right)^2 + \left[1 - \left(\frac{f_c}{f}\right)^2\right]\left[\frac{(b/a)((b/a)m^2 + n^2)}{(b^2m^2/a^2) + n^2}\right] \right\} \tag{26}$$

And for TE_{m0} modes

$$(\alpha_c)_{TE_{m0}} = \frac{R_s}{b\eta\sqrt{1 - (f_c/f)^2}} \left[1 + \frac{2b}{a}\left(\frac{f_c}{f}\right)^2\right] \tag{27}$$

Figure 8.7c shows attenuation versus frequency for TM_{11} and TE_{10} modes in rectangular copper waveguides with various side ratios b/a found using (14) and (27), respectively. It is seen that small b/a ratios give large attenuations because of the high ratio of surface to cross-sectional area.

8.8 THE TE_{10} WAVE IN A RECTANGULAR GUIDE

One of the simplest of all the waves which may exist inside hollow-pipe waveguides is the dominant TE_{10} wave in the rectangular guide, which is one of the TE modes

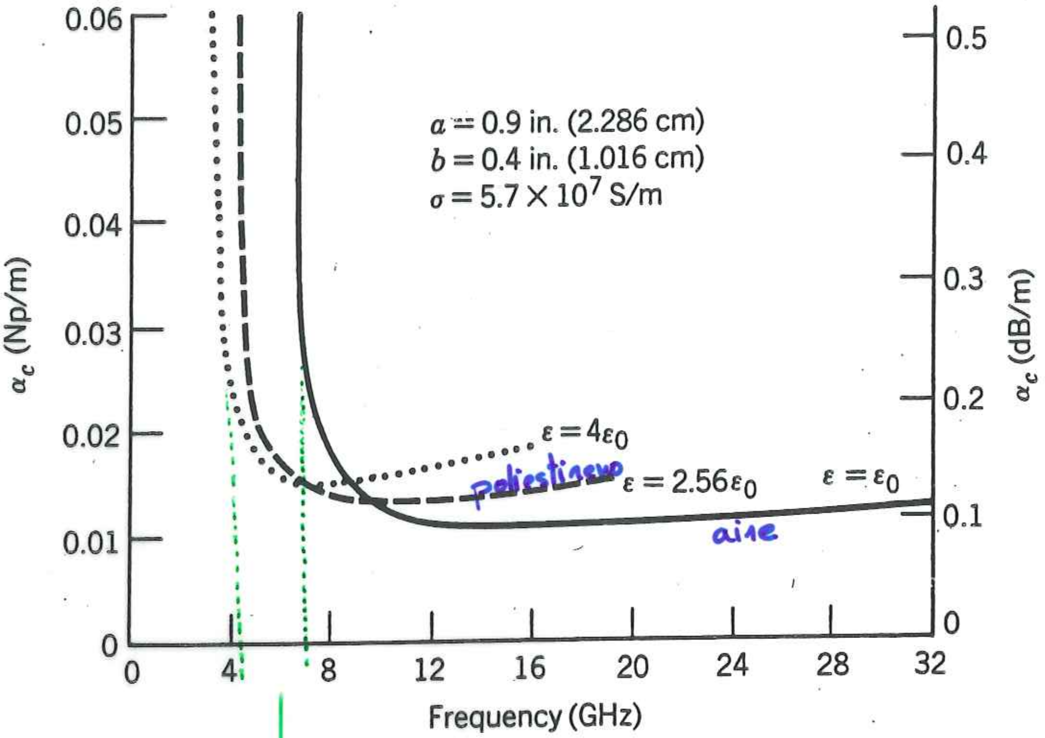

FIGURE 8-10 TE_{10} mode attenuation constant for the *X*-band rectangular waveguide.

frecuencias de corte disminuyen cuanto más "dieléctrico" es el interior de la guía.